Epigenetic dysregulation of eukaryotic initiation factor 3 subunit E (eIF3E) by lysine methyltransferase REIIBP confers a pro-inflammatory phenotype in t(4;14) myeloma

Phyllis S. Y. Chong,[1,2*] Jing Yuan Chooi,[1*] Sze Lynn Julia Lim,[2] Tae-Hoon Chung,[2] Reinhard Brunmeir,[2] Aaron Chung Yong Leow,[2] Sabrina Hui Min Toh,[2] Kalpnaa Balan,[2] Muhamad Irfan Bin Azaman,[2] Zhengwei Wu,[2,3] Nagavidya Subramaniam,[4] Leah A. Vardy[4] and Wee-Joo Chng[1,2,5]

[1]Department of Medicine, Yong Loo Lin School of Medicine, National University of Singapore; [2]Cancer Science Institute of Singapore, National University of Singapore; [3]Genome Institute of Singapore, Agency for Science, Technology and Research (A*STAR); [4]A*STAR Skin Research Labs and Skin Research Institute of Singapore, A*STAR, Immunos and [5]Department of Hematology-Oncology, National University Cancer Institute of Singapore, National University Health System, Singapore

*PSYC and JYC contributed equally as first authors.

Correspondence: W-J. Chng
mdccwj@nus.edu.sg

Received: May 2, 2023.
Accepted: December 11, 2023.
Early view: December 21, 2023.

https://doi.org/10.3324/haematol.2023.283467

Abstract

REIIBP is a lysine methyltransferase aberrantly expressed through alternative promoter usage of NSD2 locus in t(4;14)-translocated multiple myeloma (MM). Clinically, t(4;14) translocation is an adverse prognostic factor found in approximately 15% of MM patients. The contribution of REIIBP relative to other NSD2 isoforms as a dependency gene in t(4;14)-translocated MM remains to be evaluated. Here, we demonstrated that despite homology with NSD2, REIIBP displayed distinct substrate specificity by preferentially catalyzing H3K4me3 and H3K27me3, with little activity on H3K36me2. Furthermore, REIIBP was regulated through microRNA by EZH2 in a Dicer-dependent manner, exemplifying a role of REIIBP in SET-mediated H3K27me3. Chromatin immunoprecipitation sequencing revealed chromatin remodeling characterized by changes in genome-wide and loci-specific occupancy of these opposing histone marks, allowing a bidirectional regulation of its target genes. Transcriptomics indicated that REIIBP induced a pro-inflammatory gene signature through upregulation of TLR7, which in turn led to B-cell receptor-independent activation of BTK and driving NFκB-mediated production of cytokines such as IL-6. Activation of this pathway is targetable using Ibrutinib and partially mitigated bortezomib resistance in a REIIBP xenograft model. Mechanistically, REIIBP upregulated TLR7 through eIF3E, and this relied on eIF3E RNA-binding function instead of its canonical protein synthesis activity, as demonstrated by direct binding to the 3'UTR of *TLR7* mRNA. Altogether, we provided a rationale that co-existence of different NSD2 isoforms induced diversified oncogenic programs that should be considered in the strategies for t(4;14)-targeted therapy.

Introduction

Multiple myeloma (MM) is a neoplasm of plasma cells characterized by the uncontrolled proliferation of abnormal plasma cells in the bone marrow incapable of producing functional antibodies.[1] Current treatment regime involves single or combination of novel drug classes such as proteasome inhibitors (bortezomib), immunomodulatory drugs (lenalidomide) and monoclonal antibodies (daratumumab), which have significantly improved survival outcomes in patients.[2-4] However, this disease still represents an important clinical challenge as it mainly affects the elderly population and frequent development of drug resistance subsequent to initial treatment response. MM can be broadly divided into hyperdiploid and non-hyperdiploid subtypes, with the non-hyperdiploid cases identified by recurrent immnuoglobulin (Ig)G translocations such as t(4;14)(p16;q32) and t(11;14)(q13;q32) in ~15% of MM patients respectively.[5,6] Such recurrent chromosomal translocations are central to the pathogenesis of MM and predicts the treatment response and clinical outcome of the patient. Patients with t(4;14) translocation, which displays a dysregulation of the *NSD2* locus and its alternatively spliced variants, has one of the worst prognosis when compared to other biological subgroups, but represents an intermediate-risk group given its response towards bortezomib.[7,8]

We and others have sought to study the function of the protein products arising from *NSD2* gene, which includes the full-length isoform NSD2, and the shorter isoforms NSD1 and REIIBP.[9-19] NSD2 contains 1,365 amino acids, and harbors conserved motifs such as PWWP domain, PHD-type zinc fingers and HMG box which are typically found in proteins with chromatin-binding ability and recognition of histone marks. The C-terminal region resides a functional and catalytic SET domain, which is essential for the oncogenic activities of NSD2. *In vitro* and *in vivo* histone methyltransferase assays demonstrated that the primary activity of NSD2 is H3K36 dimethylation, which leads to a global gene activation reprogramming that drives myelomagenesis.[11] Other histone modifications modulated by NSD2 includes H4K20 and H3K27 methylation, as well as H3 acetylation.[12-14] Through its histone-modifying activities, NSD2 promotes cancer phenotypes such as increased cell proliferation, clonogenicity, adhesion to bone marrow stroma and tumorigenesis.[11,15-17] NSD1 is identical to the N-terminus region of NSD2 spanning 647 amino acids. Despite lacking the SET domain, it regulates gene expression through binding to the promoter of target genes such as *GLO1*, and truncation studies indicated that the HMG box at the C-terminus of NSD1 is important for this function.[18] On the other hand, the role of REIIBP, which is overexpressed independent of *NSD2* breakpoint clusters, is poorly understood.[9,10] This transcript arises from intron 9 of the *NSD2* locus and is identical to the C-terminus of NSD2 spanning 584 amino acids, retaining the SET domain.[19] Furthermore, the subcellular localization of REIIBP is found in the cytoplasm and nucleoli, which differs from NSD1 and NSD2 that reside in the nucleus.[9] Hence, it is likely that REIIBP have differential histone methylation targets as well as novel functions that are not fully elucidated, and the contribution of REIIBP relative to other NSD2 isoforms as a dependency gene in t(4;14)-translocated MM remains to be evaluated. In this study, we generated a stable cell line that overexpresses REIIBP to perform an unbiased study of the histone lysine methylation and regulatory activities of REIIBP.

Methods

Plasmids, patient samples and reagents

Full-length *NSD2, NSD1* and *REIIBP* were cloned as previously described.[11,18] Dicer and *TLR7* short hairpin RNA (shRNA) were constructed in pRP(shRNA)-EGFP-U6 vector and miR-26a, miR-31, and miR-203 were cloned in pRP[ncRNA]-Puro-CMV by VectorBuilder (USA). Two single guide RNA (sgRNA) targeting the coding region of eIF3E were cloned into vector backbone pRP(CRISPR)-Puro-hCas9-U6 and three sgRNA targeting its H3K4me3 TSS peak (VectorBuilder, USA). *EZH2* small interfering RNA (siRNA) was purchased from Thermo Fisher Scientific (USA); EPZ-6438 and GSK-126 were purchased from Selleck Chemicals (USA). Ibrutinib, bortezomib and loxoribine were purchased from Santa Cruz (USA). Patient samples were collected with written consent at the National University Cancer Institute Singapore with the approval from the Institutional Review Board (DSRB 2017/00196).

In vitro histone methyltransferase activity assay

Histone H3 tri-methyl K27 and K4 quantification kits were purchased from Abcam and performed as per manufacturer's instructions; 0, 2, 5, 10 or 20 μg of nuclear extracts (Thermo Fisher Scientific) were added to biotinylated substrate (unmethylated histone peptide) and anti-H3K27me3 or anti-H3K4me3 antibody was used for capture and readings taken at absorbance 450 nm with a microplate reader (Tecan). S-adenosylmethionine (SAM) methyltransferase assay was performed using 1 μM SAM as a methyl-group donor to modify 2 μg of H3 substrate by 2 μg REIIBP in a reaction buffer previously described[20] at 30°C for 2 hours. Proteins were resolved on 15% SDS-PAGE and probed with indicated antibodies.

Chromatin immunoprecipitation sequencing

Chromatin immunoprecipitation (ChIP) sequencing was performed on isogenic cell lines RPMI8226-Vcon and RPMI8226-REIIBP (20 million cells each) using reagents obtained from Cell Signaling Technology (SimpleChIP® Enzymatic Chromatin IP Kit) according to the manufacturer's protocol. Monoclonal antibodies used for ChIP were anti-H3K27me3 (CST, #9733) and anti-H3K4me3 (CST, #9751). DNA were extracted with MinElute PCR Purification Kit (Qiagen). More information is provided in the *Online Supplementary Appendix*.

In vivo xenograft study

In order to generate a REIIBP xenograft model, RPMI8226-REIIBP stable cells (5×10^6) were suspended in 0.1 mL phosphate-buffered saline and subcutaneously injected into the flanks of NOD/SCID female mice (6 weeks old, InVivos). Tumor growth was monitored using calipers every 3 days until a volume of 150 mm^3 (calculated as length x width [2]/2) is reached, which developed between 2-3 weeks, and randomized into four groups: dimethyl sulfoxide (DMSO) (1% final concentration), ibrutinib (15 mg/kg), bortezomib (0.4 mg/kg) and combination (N=5 mice/group). Treatment was performed every 2 days via intraperitoneal injection for 2 weeks. Tumors were harvested for weight analysis. The responsible use of animals was approved and in accordance to protocol by Institutional Animal Care and Use Committee (IACUC; National University of Singapore).

Statistical analysis

Student's *t* test was used to compare significant differences between groups using GraphPad Prism or Excel and adjusted using Benjamini-Hochberg correction method for multiple comparisons. Correlation analyses were performed between REIIBP (ENST00000382888, transcript NSD2-203

of Enesmbl annotation) and BTK in CoMMpass dataset using Pearson correlation analysis. Survival analysis was performed by Kaplan–Meier method and assessed using the log-rank test generated with MMTools. Using Wilcoxon's test, association between REIIBP expression and bortezomib response was determined in CoMMpass (IA13a version) using the drug treatment response data that had included bortezomib.

A detailed description is available in the *Online Supplementary Appendix*.

Results

REIIBP is expressed in t(4;14) myeloma cells independent of other NSD2 isoforms, *FGFR3* or *ACA11* expression and harbored oncogenic activity

In order to elucidate the biological role of REIIBP in myeloma, we first examined the endogenous expression of REIIBP in human myeloma cell lines (HMCL). We optimized an antibody that recognizes the C-terminus region of NSD2 and detected a band that corresponded to REIIBP at ~62 kDa. Using a different N-terminus antibody, we probed for NSD1 and NSD2. Consistent with previous reports, we detected the longest isoform of NSD2 in KMS11 and KMS34 cells, and these cells harbored the highest expression for NSD1 (Figure 1A). On the contrary, REIIBP expression was lower in KMS11 and KMS34, but abundantly expressed in other t(4;14)$^{+}$ cells, while the t(4;14)$^{-}$ cells showed little to null expression of REIIBP (Figure 1A). Next, we compared REIIBP transcript levels against other gene products that were reported to be associated with t(4;14) locus, namely *FGFR3* and *ACA11*,[9,21] but no clear correlation were observed (Figure 1B). Additionally, in t(4;14)$^{-}$ cells, we could detect *REIIBP* mRNA that was not translated into REIIBP protein (Figure 1A, B), suggesting a post-transcriptional regulatory mechanism of REIIBP in myeloma cells. Another MM cell line commonly used to study NSD isoforms is the TKO (translocation knockout) cells generated from parental KMS11 with the exon 7 on t(4;14) translocated *NSD2* allele deleted.[16,22] This resulted in almost undetectable protein levels of NSD1 and NSD2, and TKO cells also lacked the protein expression of REIIBP (*Online Supplementary Figure S1A*). For clinical relevance, we compared the expression of REIIBP in primary patient samples with varying t(4;14) status. While REIIBP protein was detected in all t(4;14) myeloma samples, it was found in only one of three non-t(4;14) samples (Figure 1C; *Online Supplementary Figure S1B*). Using shRNA targeting different regions of NSD2, we found that complete abrogation of NSD2 drives a compensatory increase in REIIBP to partially rescue cell viability (Figure 1D; *Online Supplementary Figure S1C*). These data revealed the regulatory complexity among isoforms of NSD2 in t(4;14) myelomagenesis.

We engineered RPMI8226 to stably overexpress His-tagged REIIBP given its low expression of all NSD2 isoform products (Figure 1E). In consideration of its proposed role as a histone methyltransferase, we checked whether REIIBP could be found in the nucleus. Ectopic and endogenous REIIBP were detected in both the nuclear and cytoplasmic compartments of the cell (Figure 1F; *Online Supplementary Figure S1D*). This contrasts with the exclusive expression of NSD1 and NSD2 in the nucleus. Compared to control, overexpression of REIIBP promoted myeloma cell growth in a short-term viability assay (Figure 2A) and a significant increase in soft agar clonogenic growth (Figure 2B). These were attributed to changes in cell-cycle progression (Figure 2C) with little effect on apoptosis (*Online Supplementary Figure S1E*). In order to exclude cell line-specific observations, we transiently overexpressed REIIBP in two other t(4;14)$^{-}$ cells, KMS12BM and U266, where REIIBP similarly promoted cell viability (*Online Supplementary Figure S1F*). Unlike NSD2,[7,8] overexpression of REIIBP rendered RPMI8226 cells less sensitive towards bortezomib treatment (Figure 2D). In MMRF CoMMpass clinical dataset, REIIBP contributed to poorer response towards bortezomib-based regimen, where its expression was highest in progressive disease (PD) compared with the others in a six-level description (Figure 2E). The differences in REIIBP expression was also pronounced in a two-level segregation of negative *versus* positive bortezomib response groups (Figure 2F). Taken together, REIIBP conferred growth advantage to myeloma cells and modulated bortezomib response.

REIIBP is a functional histone methyltransferase with activity on histone 3 lysine 27 and lysine 4 trimethylation *in vitro* and *in vivo*

In order to determine the effects of REIIBP on histone methylation, we evaluated its substrate specificity by performing an *in vitro* histone methyltransferase assay using the methyl donor S-adenosylmethionine (SAM), substrate H3 and purified REIIBP (*Online Supplementary Figure S2A*). After incubation, the methylated products were visualized by immunoblot. We first performed the assay using bacterial cell extracts[23] where we expressed a recombinant GST-tagged REIIBP, and detected specific modifications on H3K27me3 and H3K4me3 (*Online Supplementary Figure S2B*). As bacterially purified enzymes might not be fully activated either due to absence of post-translational modifications or other mammalian complex proteins, we repeated with 293T-purified REIIBP and confirmed the catalyzation of methylation on H3K27, H3K4 and H3K79 residues (Figure 3A). In order to rule out the possibility of contamination with other histone-modifying enzymes, we probed for EZH2 that catalyzes H3K27me3[24] and H3K79 methyltransferase DOT1L,[25] which were both undetected in the extracts (Figure 3A). We performed further validation by directly measuring the enzymatic activity of nuclear extracts from the isogenic cells in a specific H3K27 or H3K4 histone methyltransferase reaction, where increased activity was observed with REIIBP

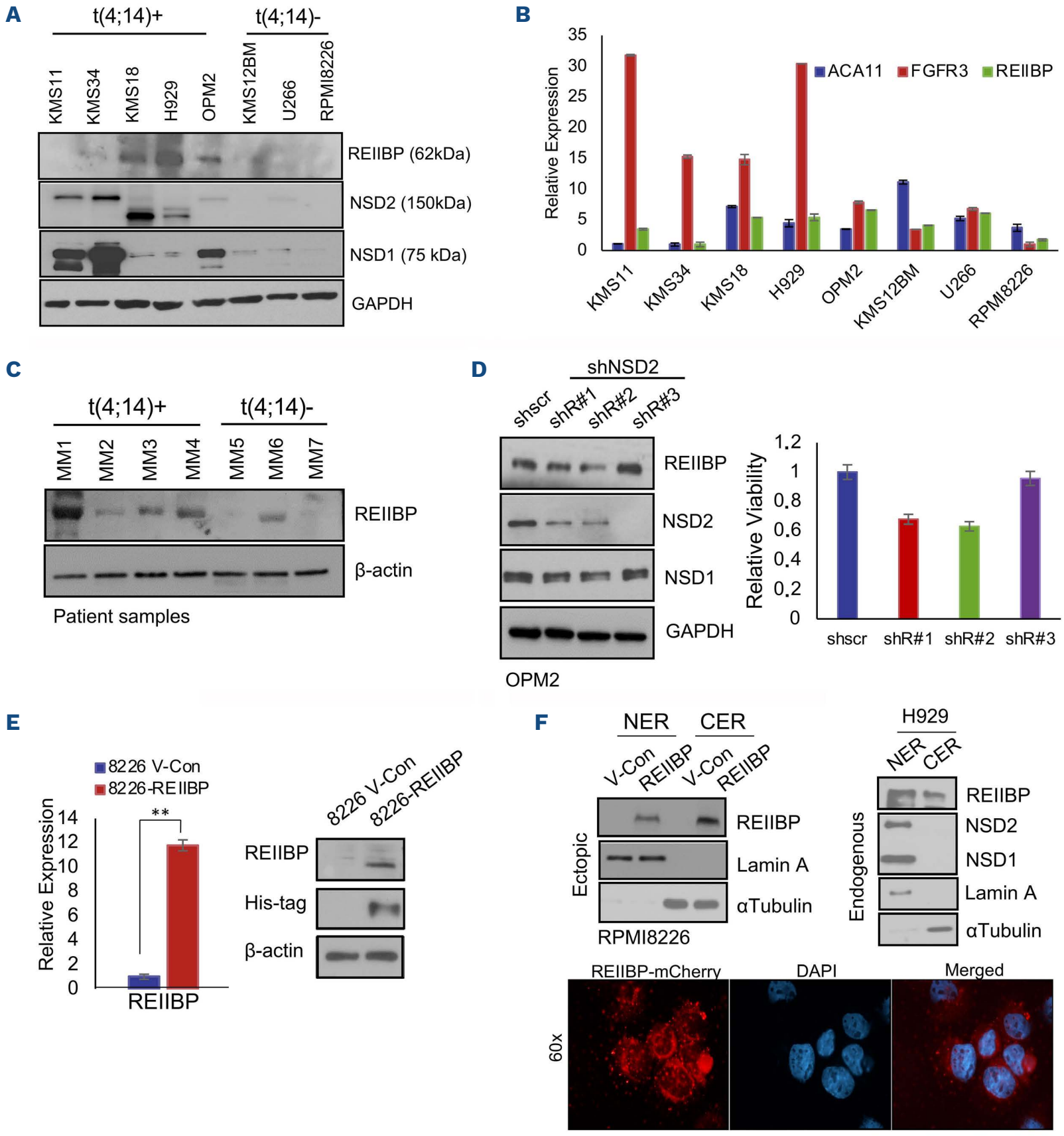

Figure 1. Expression status of REIIBP in myeloma cell lines and primary specimens. (A) Western blotting (WB) to determine the endogenous expression of NSD1, NSD2 and REIIBP in a panel of human myeloma cell lines. GAPDH was used as loading control. N=2, biological repeats, representative blots are shown. (B) Quantitative real time polymerase chain reaction (qRT-PCR) analysis of ACA11, FGFR3 and REIIBP in a panel of human myeloma cell lines. GAPDH was used as for normalization. N=3, biologically independent replicates with technical duplicates. (C) Myeloma cells from 7 patient samples with t(4;14) or non-t(4;14) status were extracted for protein and used to probe for REIIBP expression. β-actin is used for loading control. Details of patient samples can be found in *Online Supplementary Figure S1B*. (D) t(4;14)-positive cell line OPM2 was transiently transfected with NSD2 #1, #2 or #3 short hairpin RNA (shRNA) using the Neon transfection system. Cell viability was determined at 24 hours post-transfection (right) while immunoblotting with the indicated antibodies was performed at 48 hours post-transfection (left). Analysis from 3 biological repeats with technical octuplicates for CTG and representative images from 2 biological repeats for WB. The shRNA sequences can be found in the *Online Supplementary Appendix*. (E) Overexpression of REIIBP in RPMI8226 cells was determined using qRT-PCR (N=3) and WB (N=2). REIIBP expression vector contained His-tag and β-actin was used as loading control. Pairwise comparison between control and treatment group using Student's *t* test (**P<0.01). (F) Ten million RPMI8226 V-Con or REIIBP cells (ectopic expression of REIIBP, left) or H929 (endogenous REIIBP, right) were lysed to extract the nuclear (NER) and cytoplasmic (CER) protein fractions. Minimal cross-contamination was confirmed with nuclear marker lamin A and cytoplasmic marker α-tubulin. NSD1 and NSD2 were found in the nucleus as previously reported. N=2, biological repeats, representative WB are shown. (Bottom) Immunoflorescence confocal microscopy images of REIIBP-mCherry expression (red florescence) in RPMI8226 cells at 60x magnification. Nuclei were stained with DAPI (blue). Image shown is a representative field.

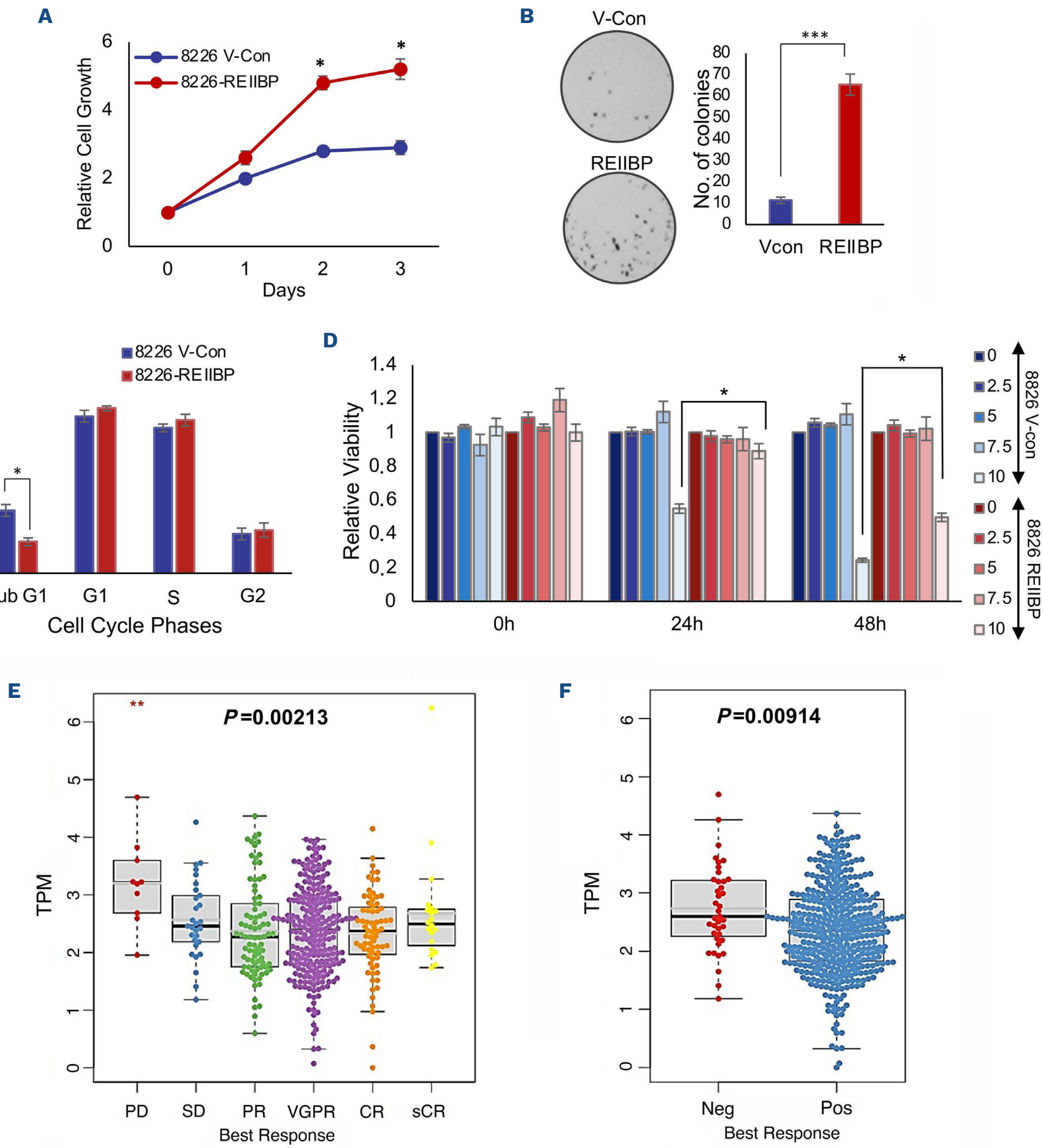

Figure 2. REIIBP is required for cell growth and conferred bortezomib resistance. (A) Cell viability was determined over 72 hours in RPMI8226 control and REIIBP-overexpressing cells and normalized against 0 hours. Three biological repeats with technical octuplicates, paired *t* test was performed to compare the means between REIIBP overexpressing with corresponding control (*P<0.05). (B) Colony-forming assay was performed to determine the long-term viability of RPMI8226 control and REIIBP-overexpressing cells over 2 weeks and the number of colonies was plotted. Representative images from 3 biological replicates and Student's *t* test indicates significance (***P<0.001). (C) Cell cycle analysis of RPMI8226 control and REIIBP-overexpressing cells were measured using flow cytometry and the percentage of cells in sub-G1, G1, S or G2/M were indicated (N=3, independent replicates). Asterisks represent significant differences (*P<0.05; Student's *t* test). (D) RPMI8226-vector control (VCon) and RPMI8226-REIIBP cells were treated with increasing concentrations of bortezomib (0, 2.5, 5, 7.5, 10 nM) and viability was determined at 24 and 48 hours using CTG assay. Viability was normalized against 0 nM and *P<0.05; Student's *t* test. Experiments were performed with 3 biological repeats with technical octuplicates. (E) REIIBP expression by 6-level best response to bortezomib without t(4;14) cases in CoMMpass dataset. PD (progressive disease: 1.6%, 12/745), SD (stable disease: 6.3%, 47/745), PR (partial response: 17.4%, 130/745), VGPR (very good partial response: 51.9%, 387/745), CR (complete response: 18.7%, 139/745), sCR (stringent complete response: 4%, 30/745). (F) REIIBP expression by 2-level best response to bortezomib without t(4;14) cases in CoMMpass dataset. Negative (PD + SD: 7.9%, 59/745) and positive (PR + VGPR + CR + sCR: 92.1%, 686/745).

overexpression in a dose-dependent manner (Figure 3B). In order to complement the *in vitro* enzymatic assays, we did a series of *in vivo* immunoblot screenings of histone methylation marks. REIIBP increased the global abundance of H3K4, H3K9, H3K27 and H3K79 trimethylation, with minimal effects on dimethylation (*Online Supplementary Figure S2C*). In order to identify SET-dependent modifications, we transfected the cells with SET domain point mutant, which

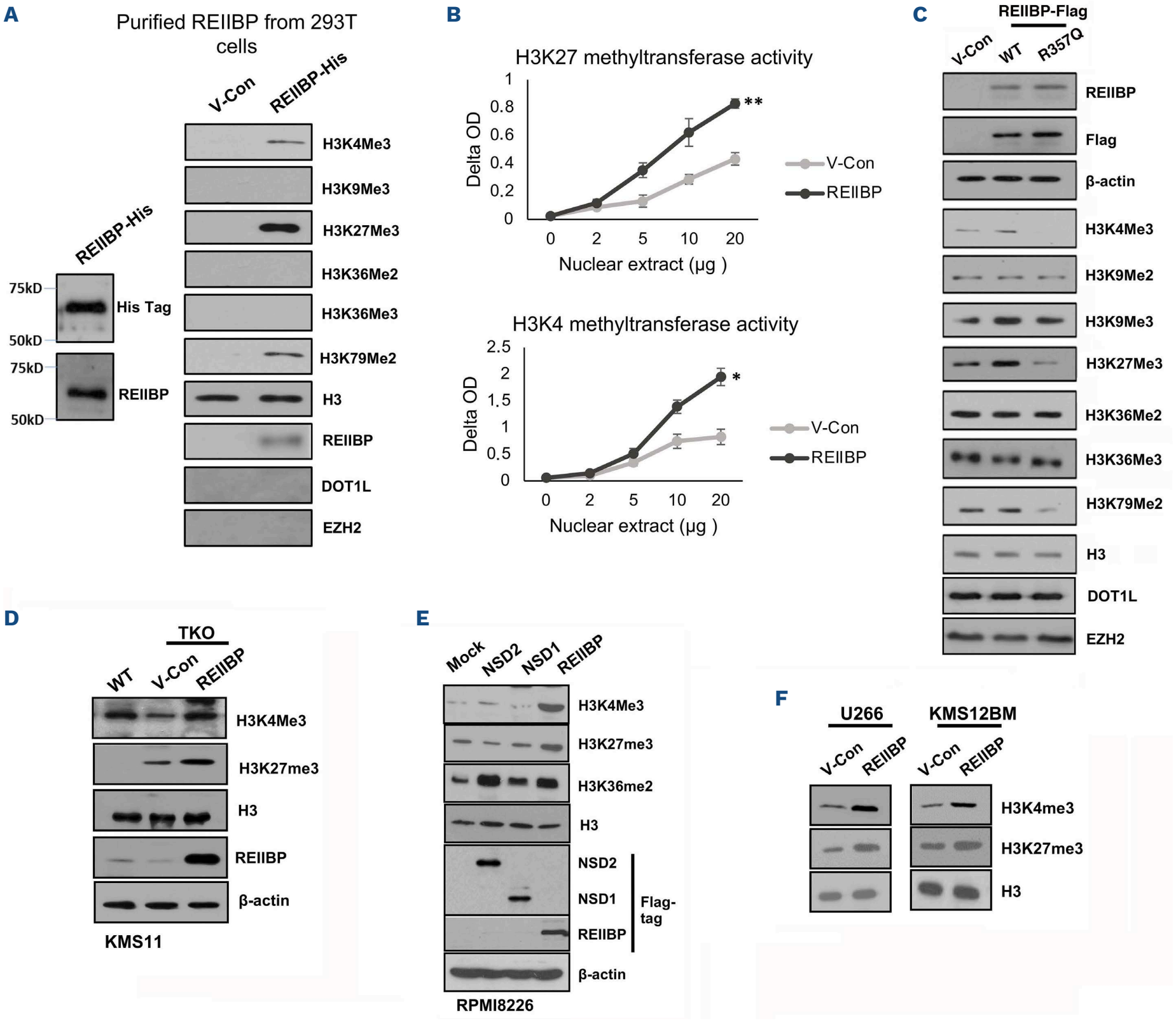

Figure 3. *In vitro* and in *vivo* histone methyltransferase assay confirm that REIIBP has a direct effect on histone methylation. (A) Purified REIIBP methyltransferase from 293T cells was added to SAM and H3 substrate in PKMT buffer. Western blotting (WB) was performed with the indicated antibodies. (B) H3K27 methyltransferase activity assay (top) was performed using increasing amount of nuclear extract from RPMI8226-vector control (VCon) or RPMI8226-REIIBP cells and readings were taken at 450 nm. N=3, biological replicates, $^{**}P<0.01$, Student's *t* test. H3K4 methyltransferase activity assay (bottom) was performed using increasing amount of nuclear extract from RPMI8226-VCon or RPMI8226-REIIBP cells and readings were taken at 450 nm. N=3, biological replicates, $^{*}P<0.05$, Student's *t* test. (C) VCon wild-type (WT) REIIBP and R357Q mutant REIIBP were transiently transfected into RPMI8226 cells and 50 µg of protein lysate were used for WB with the indicated antibodies. H3 and β-actin are the loading control. (D) KMS11 and KMS11-TKO (translocation knockout) cells transiently transfected with VCon or WT REIIBP and were used for WB with the indicated antibodies. H3 and β-actin are the loading control. (E) RPMI8226 cells were transfected with NSD1, NSD2 and REIIBP expression vectors and WB with the indicated antibodies. H3 and β-actin are the loading control. Flag-tag antibodies demonstrated equal expression of the isoforms. (F) U266 and KMS12BM transiently transfected with REIIBP expression vector from *Online Supplementary Figure S1B* were used to probe for histone marks. H3 is the loading control. All immunoblots were performed with 2 biological repeats and a representative experiment was shown.

saw an efficient abolishment of H3K4me3 and H3K27me3 histone marks (Figure 3C). Next, we reconstituted the expression of REIIBP in KMS11 TKO cells. It is notable that TKO cells had a higher expression of H3K27me3 than wild-type (WT), which is supported by previous findings that NSD2 induced a downregulation of H3K27me3.[13] Despite this, there was a consistent increase in both H3K27me3 and H3K4me3 modifications by REIIBP (Figure 3D). As a direct comparison of the catalytic activities among NSD2, NSD1 and REIIBP, we overexpressed these proteins in parallel. We observed the most significant increase in H3K36me2 by NSD2, as expected.[11] Conversely, H3K27me3 and H3K4me3 were increased by REIIBP, but not NSD1 or NSD2 (Figure 3E). These modifications by REIIBP were reproducible in other myeloma cell lines (Figure 3F; *Online Supplementary Figure S2D*). Collectively, we demonstrated a SET-dependent activity of REIIBP on H3K4 and H3K27 trimethylation but not NSD2-associated H3K36me2.

EZH2 is an upstream regulator of REIIBP and is mediated through microRNA

EZH2 is a key H3K27me3 enzyme, and previous reports linked EZH2 upstream of NSD2.[13,26] In order to define the relationship between REIIBP and EZH2, we first checked the expression of EZH2 in our isogenic cells. Similar levels of EZH2 suggested that the upregulation of H3K27me3 is unlikely attributed to a modulation of EZH2 levels (*Online Supplementary Figure S3A*). Next, we overexpressed REIIBP in a K562-EZH2 null cell line (*EZH2*$^{\Delta/\Delta}$), which led to a restoration of H3K27me3 levels, albeit with dose-limiting effect

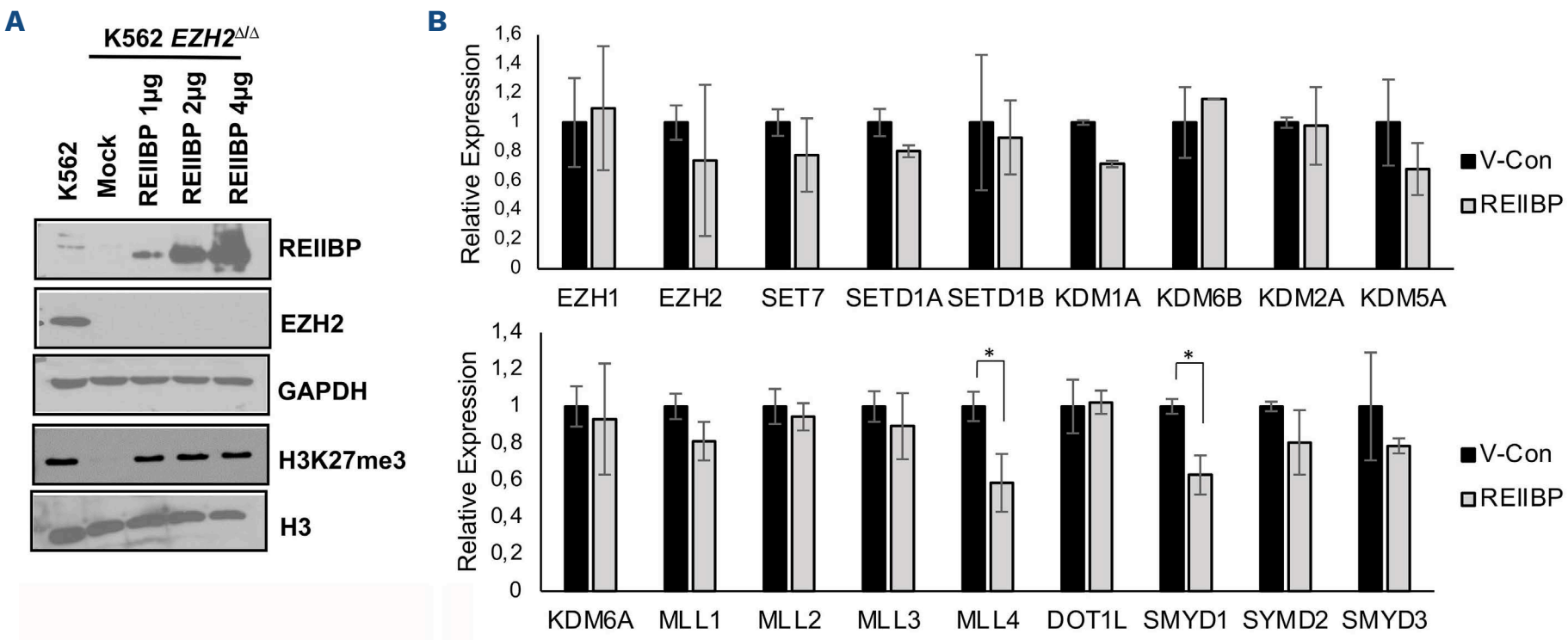

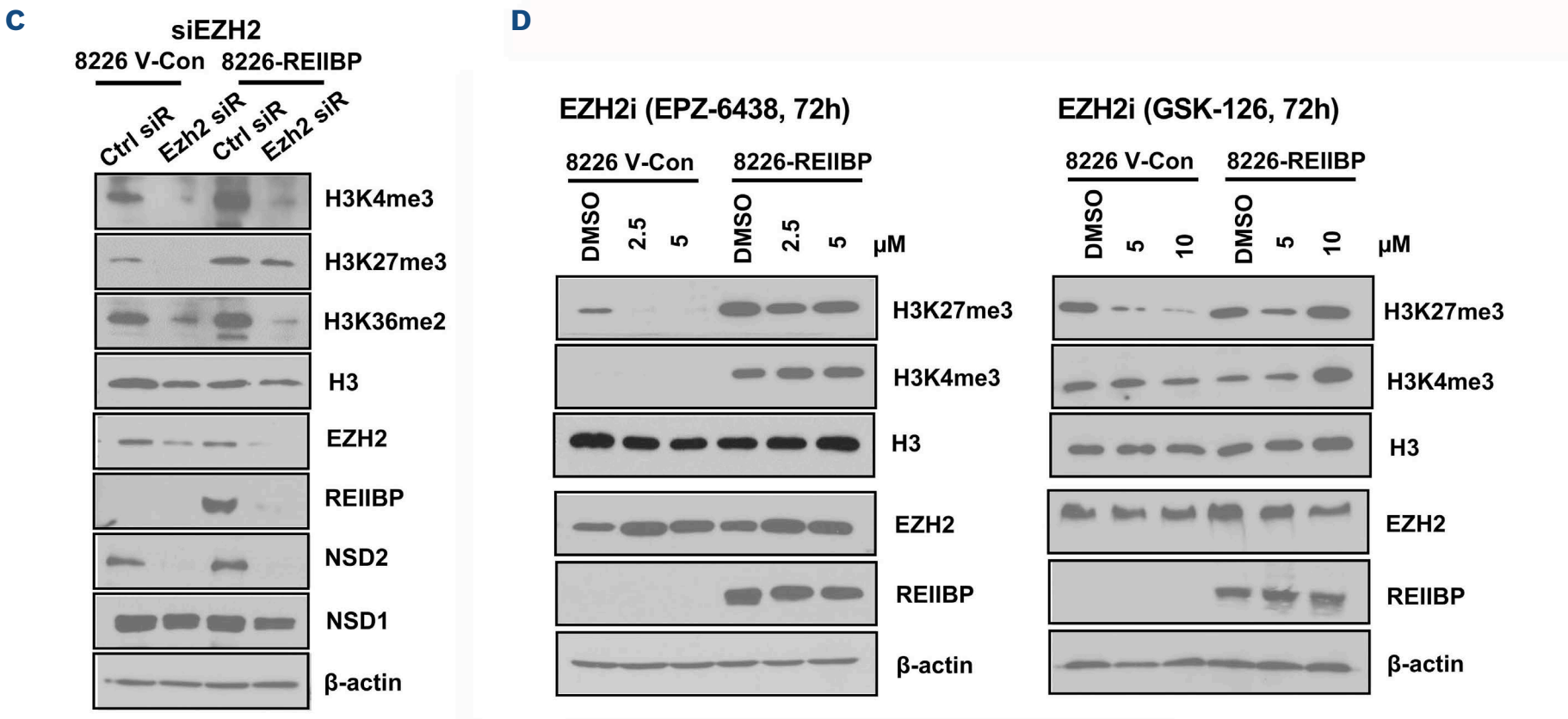

Continued on following page.

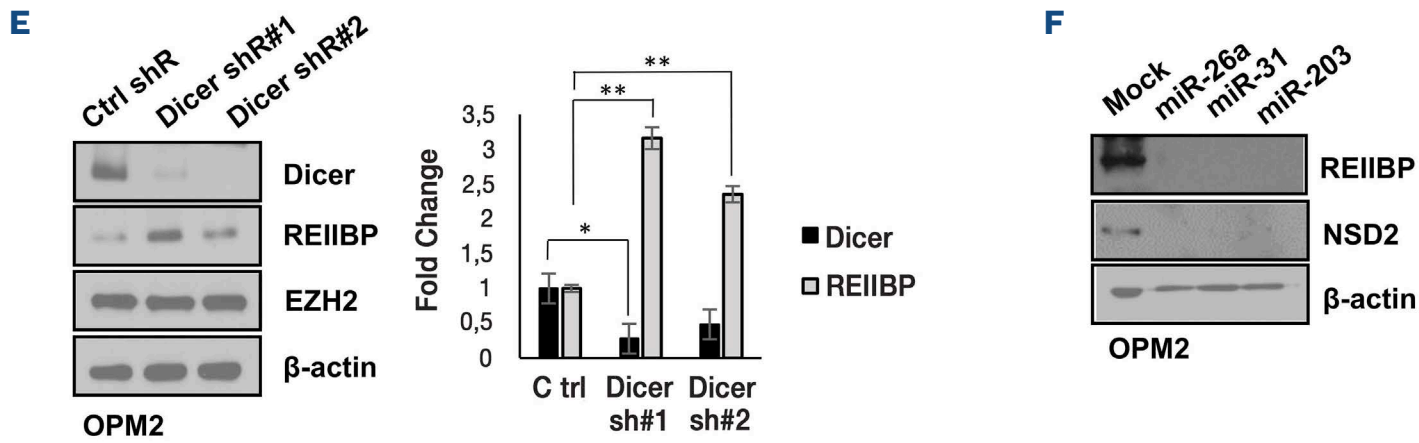

Figure 4. REIIBP regulates H3K27me3 independent of EZH2. (A) K562 EZH2$^{\Delta/\Delta}$ cells were transiently transfected with increasing amounts of REIIBP plasmid and protein were extracted at 48 hours to determine the levels of H3K27me3. GAPDH and H3 are the loading controls. N=2, independent replicates. (B) Gene expression of a panel of histone methyltransferases and demethylases were determined in RPMI8226-vector control (VCon) and RPMI8226-REIIBP cells. GAPDH was used for normalization. N=3, biologically independent replicates with technical duplicates. Asterisks represent significant differences (*P<0.05) determined by Student's t test. (C) RPMI8226-VCon and RPMI8226-REIIBP cells were transiently transfected with control or EZH2 small interfering RNA (siRNA) (100 nM) and protein harvested at 48 hours for western blotting (WB) with the respective antibodies. H3 and β-actin are the loading control (N=2, biological replicates). (D) RPMI8226-VCon and RPMI8226-REIIBP cells were treated with 2 EZH2 inhibitors, EPZ-6438 (left) and GSK-126 (right), for 72 hours before protein was harvested for WB (N=2, biological replicates, representative WB). H3 and β-actin are the loading control. (E) 1x10^6 OPM2 cells were transiently transfected with 2 μg of scrambled short hairpin RNA (shRNA), Dicer shRNA #1 or #2 for 48 hours and protein lysate was harvested. WB was performed with the indicated antibodies (N=2, biological replicates, representative WB). β-actin is the loading control. Transfection for 24 hours was harvested for mRNA and shown as fold change relative to scrambled shRNA control. N=3, biologically independent replicates with technical duplicates. Asterisks represent significant differences (*P<0.05; **P<0.01) determined by Student's t test and Benjamini-Hochberg correction method was applied for multiple comparisons. (F) OPM2 cells were transiently transfected with 75 nM of miRNA-26, miRNA-31 or miRNA-203 for 48 hours and the protein levels of REIIBP and NSD2 were determined. N=2, independent replicates.

in the complete absence of EZH2 (Figure 4A). We further checked a panel of other histone methyltransferases and demethylases. Most were unchanged except for downregulation, and not upregulation, of H3K4 methyltransferases MLL4 and SMYD1 (Figure 4B). Overall, these data indicated that H3K27 and H3K4 trimethylation mediated by REIIBP were independent of other enzymes.

Next, we inhibited EZH2 via two different mechanisms, siRNA-mediated abrogation of EZH2 levels, and pharmacological inhibitors (EPZ-6438 and GSK-126) known to affect EZH2-mediated H3K27me3 but leave EZH2 levels unchanged.[27] Knockdown of EZH2 showed an almost complete abrogation of NSD2 and H3K36me2, thus acting as a positive control in our system. Notably, REIIBP was also abrogated but not NSD1, and REIIBP-associated H3K4me3 and H3K27me3 were reduced (Figure 4C). This indicated that EZH2 not only regulated NSD2, but REIIBP as well, and such regulation occurred at both the mRNA and protein levels (*Online Supplementary Figure S3B*). Treatment with EZH2 inhibitors (EZH2i) provided alternative insights as it reduced H3K27me3 levels in WT cells but not in REIIBP-overexpressing cells (Figure 4D). The residual H3K27me3 confirmed that REIIBP could modulate H3K27me3 levels that was not targetable by EZH2 inhibition. EZH2i did not affect REIIBP levels and correspondingly, H3K4me3. The observation that siEZH2 but not EZH2i affected REIIBP would suggest that EZH2 protein rather than its enzymatic activity is required for REIIBP regulation.

One reported mechanism through which EZH2 regulated NSD2 is by microRNA (miRNA).[26] Given the identical 3'UTR of NSD2 and REIIBP, this prompted us to examine whether REIIBP is likewise regulated by miRNA and identify the specific miRNA that might be targeting REIIBP. For this purpose, we performed the subsequent miRNA experiments in OPM2 which harbored the 3'UTR region on endogenous REIIBP. Depletion of Dicer using two independent shRNA rescued the mRNA and protein levels of REIIBP (Figure 4E), and was reproducible in RPMI8226 (*Online Supplementary Figure S3C*). There were other cell lines whereby Dicer knockdown led to a downregulation of EZH2, resulting in the depletion of REIIBP (*Online Supplementary Figure S3D*), reinforcing our hypothesis that EZH2 was upstream of REIIBP. Lastly, we overexpressed the three EZH2 miRNA that were previously reported to target the 3'UTR of *NSD2* gene,[26] namely miR-26a, miR-31, and miR-203. These miRNA resulted in the abrogation of both NSD2 and REIIBP levels (Figure 4F). Altogether, we demonstrated a connection of REIIBP to EZH2 histone methyltransferases network, although REIIBP catalytic activity on H3K27me3 was independent of EZH2.

Transcriptomics identified a novel role of REIIBP in pro-inflammatory processes through activation of TLR7-BTK-IL6 pathway

Previously, we reported that NSD2 is involved in the regulation of cell growth, adhesion and Wnt signaling pathways.[28] In order to gain insights into the transcriptional program induced by REIIBP, we performed gene expression profiling (Figure 5A; *Online Supplementary Table S1*). Upon REIIBP

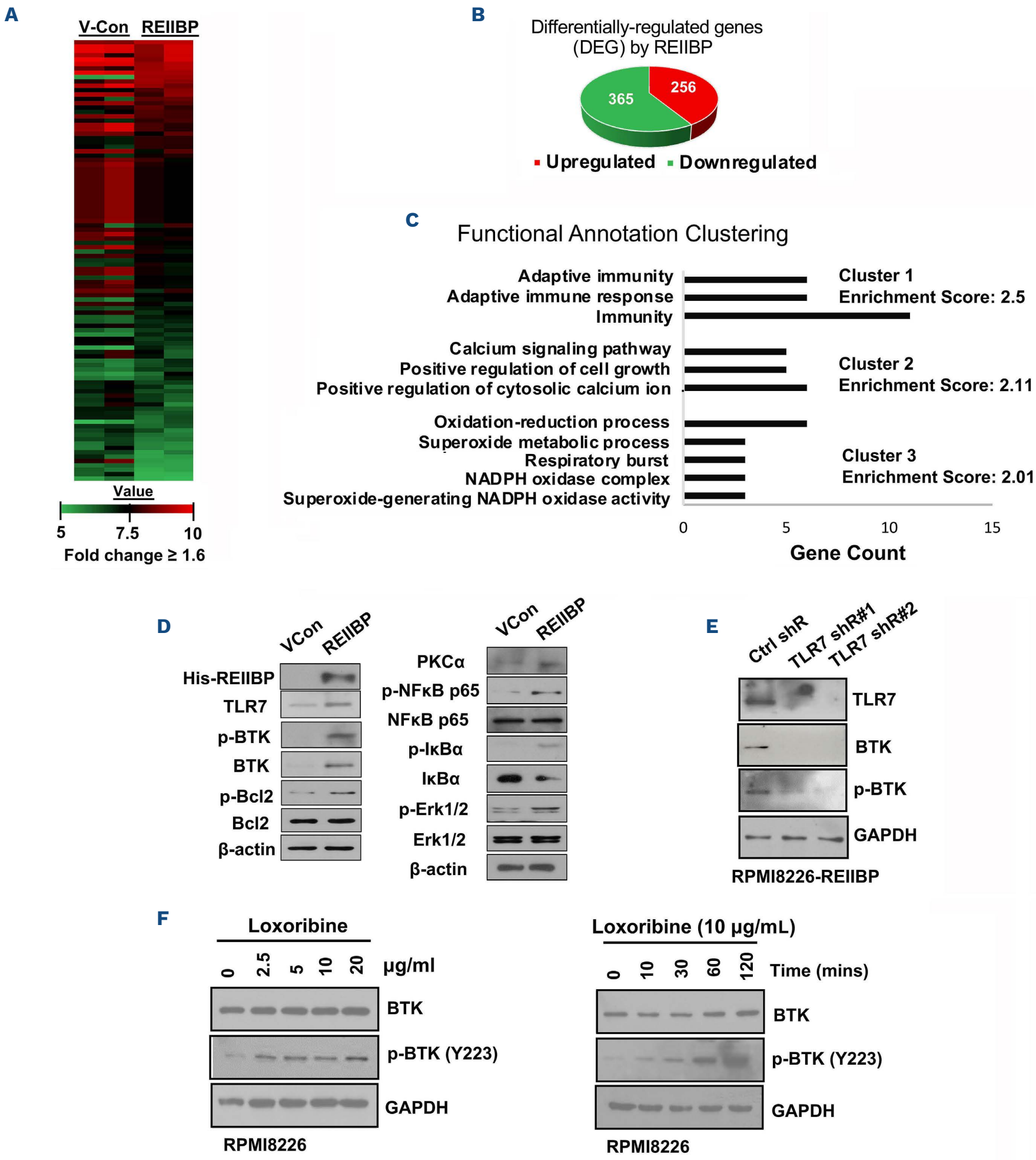

Figure 5. Global transcriptional changes in REIIBP-overexpressing cells. (A) Heat map of genes with log fold-change cutoff of 1.6 were shown. See *Online Supplementary Table S1* for microarray data. N=2, independent replicates. (B) Up- and downregulated genes were plotted as a pie chart. (C) Functional annotation clustering was performed using DAVID Bioinformatics Resources[49] with the differentially expressed genes (DEG). The processes with the top 3 enrichment scores are presented. The x-axis represents the number of genes, while the y-axis represents the ontology categories. (D) 50 μg of protein lysate from RPMI8226-vector control (VCon) and RPMI8226-REIIBP cells were used to probe with the indicated antibodies in TLR7-BTK-NF-kB activation pathway. β-actin is the loading control (N=2, biological repeats, representative western blot [WB] shown). (E) RPMI8226-REIIBP cells were transiently transfected with 2 TLR7-targeting short hairpin RNA (shRNA) and protein harvested 48 hours post-transfection. WB was performed with the indicated antibodies (N=2, biological repeats, representative WB shown). GAPDH is the loading control. (F) RPMI8226 cells were treated with increasing concentration of loxoribine for 60 minutes (left) or increasing duration at fixed concentration of 10 μg/mL (right). Phospho-BTK and total BTK levels were determined using WB and GAPDH is the loading control (N=2, biological repeats, representative WB shown).

overexpression, there were 365 downregulated and 256 upregulated genes (Figure 5B). The differentially expressed genes (DEG) were subjected to gene ontology analysis to reveal an enrichment in processes such as response to stimuli, cell growth and metabolism (Figure 5C), and the top five upregulated genes (*CYBB, TLR7, FAIM3, BTK, PDIA2*) were independently validated (*Online Supplementary Figure S4A*). Amongst these, Toll-like receptor 7 (TLR7) seems to be of particular relevance given its role in cytokine production to promote the survival and drug resistance of myeloma cells.[29] Interestingly, we also observed the concerted upregulation of BTK, a putative downstream target of TLR,[30] together with activation of its downstream effector protein phospho-NFκB[31-33] (Figure 5D; *Online Supplementary Figure S4B*). shRNA-mediated gene silencing of TLR7 reduced both BTK and phospho-BTK (Figure 5E), while stimulation with a TLR7 agonist, loxoribine, phosphorylated BTK in myeloma cells in a dose- and time-dependent manner (Figure 5F). These suggested that in the absence of BCR in myeloma cells, TLR7 can be an alternative upstream receptor for a fully activated, phosphorylated BTK. Next, we measured the levels of pro-inflammatory cytokines and found a significant dysregulation of cytokine gene expression, particularly interleukin (IL)-6 (Figure 6A). This was coupled with increased secretion of IL-6 into the supernatant by the myeloma cells (Figure 6B). In order to assess whether REIIBP cells were dependent on BTK activation, we treated HMCL with ibrutinib.[34-37] t(4;14)-positive OPM2, H929 and KMS18 with high levels of REIIBP were significantly inhibited as compared to KMS11 and KMS34 harboring lower REIIBP, while t(4;14)-negative U266 was most resistant (Figure 6C). This was confirmed in the RPMI8226 isogenic system where REIIBP expression segregated ibrutinib response (*Online Supplementary Figure S5A-C*). Moreover, the inhibitory effects of ibrutinib were potentiated in combination with bortezomib (*Online Supplementary Figure S6A-C*). *In vivo*, NSG mice engrafted with REIIBP cells developed tumors more efficiently than vectro control (VCon) and randomized treatment with ibrutinib-bortezomib combination demonstrated superior efficacy to single drug or DMSO control groups (Figure 6D, E). Our observations corroborated with Cancer Cell Line Encyclopedia (CCLE) and DepMap resources showing BTK dependency in MM (*Online Supplementary Figure 7A, B*). In patient datasets, TLR7 and BTK were associated with poor overall survival (*Online Supplementary Figure 7C, D*), and demonstrated correlation between their expression profiles (*Online Supplementary Figure S7E*).

Altered occupancy of H3K4me3 and H3K27me3 revealed the complexity in the bidirectional regulation of genes by REIIBP

In order to assemble our findings on how REIIBP histone modifications contributed to its transcriptional profile, we next performed genome-wide mapping of H3K4me3 and H3K27me3 using ChIP sequencing. Consistent with their increased levels, the distribution of H3K4me3 was significantly enriched near the TSS upon REIIBP overexpression, while H3K27me3 signal was relatively flat across 5 kb region before and after TSS, with some focal enrichment at TSS (Figure 7A). Differential H3K4me3 and H3K27me3 peaks were subjected to gene ontology (*Online Supplementary Figure S8A*) and KEGG analysis to reveal enrichment in pathways such as PI3K-Akt signaling and metabolism (*Online Supplementary Figure S8B*), and their occupancy were analyzed with DREME motif discovery (*Online Supplementary Figure S8C*). Comparison of the genomic distributions indicated an expansion of H3K4me3 and H3K27me3 peaks into intergenic regions with reduced weightage on promoters (*Online Supplementary Figure S8D*). Next, we performed a *t* test of occupancy values across the whole genome to identify a list of genes whose distribution for H3K4me3 and H3K27me3 were significantly altered by REIIBP (*Online Supplementary Table S2*). There were 328 H3K4me3 and 1,256 H3K27me3 altered genes respectively, and 45 overlapping gene loci that were doubly marked (*Online Supplementary Figure S8E*). In consideration that H3K4me3 functions as a permissive histone mark that opposes H3K27me3, we sought to examine the impact of how their loss or gain affected gene expression. We found a clear association between increased H3K4me3 occupancy with upregulated transcription, but H3K27me3 peaks did not necessarily function as silencers to repress gene expression (Figure 7B). A different trend was observed with the doubly marked genes, where the effect of H3K4me3 on promoting expression is of a lesser extent. In this group, high levels of H3K27me3 could block the expression of genes despite H3K4me3 occupancy, indicating that lowering H3K27me3 is a prerequisite for expression. Accordingly, the group with H3K4me3^{high}/H3K27me3^{low} demonstrated the highest transcriptional activity. Overall, our data indicated a dynamic and complex control through the balance of H3K4me3 and H3K27me3 histone modifications on fine-tuning transcription.

REIIBP upregulates TLR7-BTK pathway through eIF3E

We performed integrative analysis of transcriptomics and ChIP-sequencing datasets, and identified eIF3E whose elevated expression can be attributed to H3K4me3 occupancy at its transcriptional start site. To ascertain this, we designed three sgRNA and used CRISPR/Cas9 editing for precise deletion of the H3K4me3 peak, and this led to the reduction in eIF3E levels (Figure 8A). Upregulation of eIF3E by REIIBP is conserved in other HMCL (*Online Supplementary Figure S9A*) and associated with disease progression and adverse prognosis (*Online Supplementary Figure S9B*). Next, we assessed whether and if so, how eIF3E contributed to REIIBP and its pro-inflammatory phenotype. Depletion of eIF3E significantly impaired growth of REIIBP cells in viability and clonogenic assays (*Online Supplementary Figure S9C-E*), and suppressed the expression of TLR7 and BTK (*Online Supplementary Figure S9F*). Given

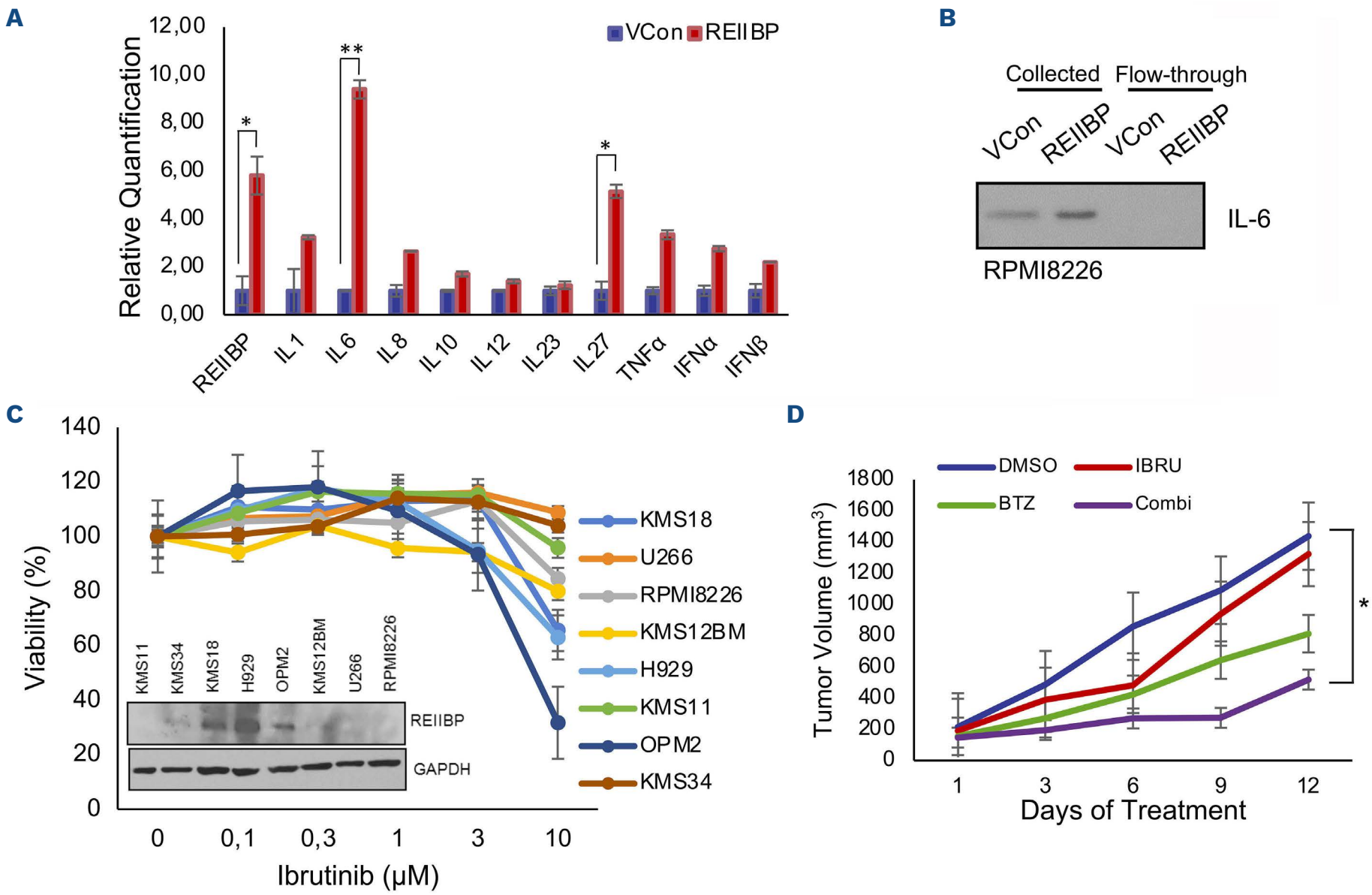

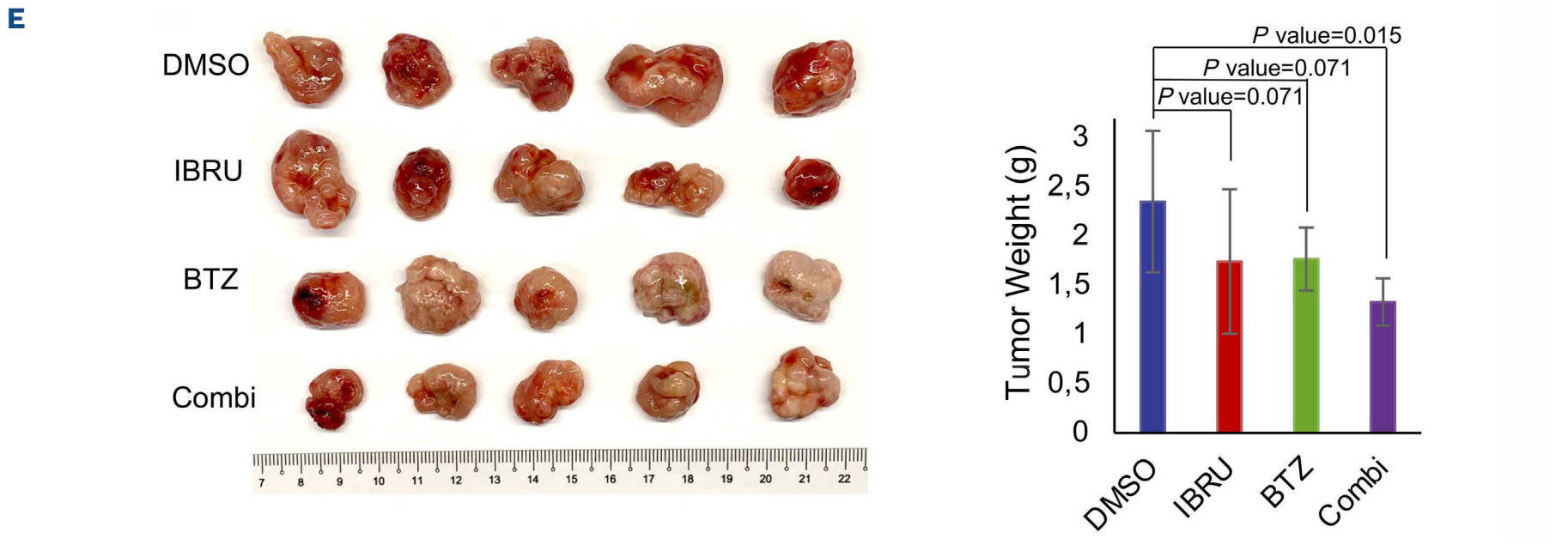

Figure 6. Ibrutinib potentiates the inhibitory effects of bortezomib. (A) The mRNA expression of multiple cytokines and chemokines were determined in RPMI8226-vector control (VCon) and RPMI8226-REIIBP cells by quantitative real time polymerase chain reaction (qRT-PCR). GAPDH was used for normalization. N=3, biologically independent replicates with technical duplicates. Asterisks represent significant differences (*P<0.05; **P<0.01) determined by Student's t test. (B) Interleukin (IL)-6 in the cell culture supernatant was collected from filter unit and flow-through, and measured by western blotting (WB) in RPMI8226-VCon and RPMI8226-REIIBP cells (N=2, biological repeats, representative WB shown). (C) Panel of myeloma cell lines were treated with increasing concentrations of ibrutinib (IBRU) for 48 hours and viability was plotted (3 biological repeats with technical octuplicates) relative to control (100%). The expression of REIIBP from Figure 1A is included as reference. (D) Xenografts of RPMI8226-REIIBP (5 million cells) were allowed to grow for 3 weeks until desired size, and treatment with 1% dimethyl sulfoxide (DMSO), 20 mg/kg ibrutinib, 0.4 mg/kg bortezomib (BTZ) or combination proceeded for 12 days with measurement of tumors with calipers. N=5, biological repeats. Asterisks represent significant differences (*P<0.05; Student's t test) between DMSO control and Combi group. (E) Tumors were harvested and weighed in grams. The P values were indicated in the figure by performing Student's t test, comparing each treatment with DMSO control. Harvested tumors were photographed.

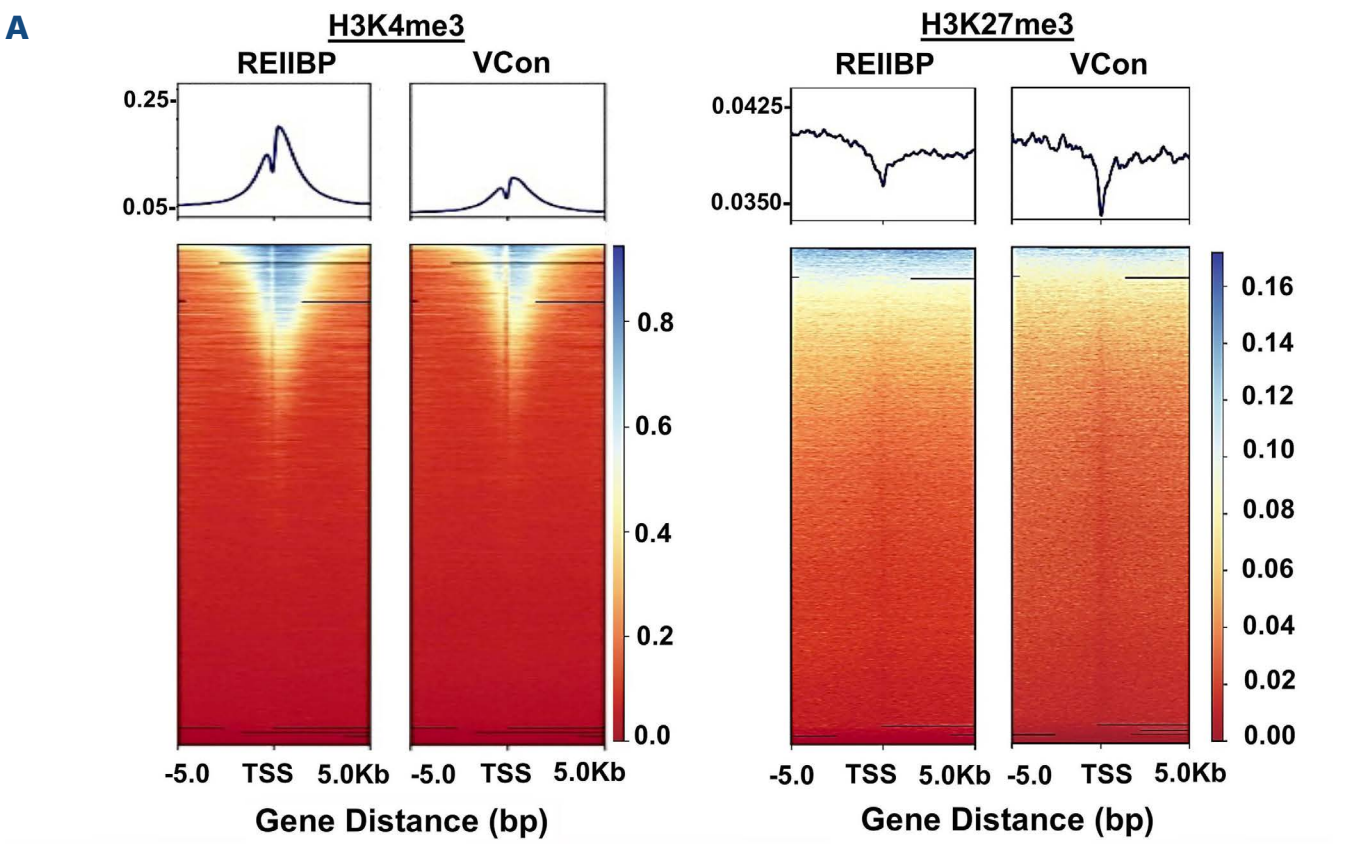

Figure 7. Chromatin immunoprecipitation sequencing of H3K4me3 and H3K27me3 revealed dynamic gene regulatory mechanisms by REIIBP. (A) Heatmap of averaged H3K4me3 and H3K27me3 signals enrichment on genomic loci at TSS from 3 biological replicates of chromatin immunoprecipitation (ChIP)-sequencing analysis was shown and normalized to the corresponding inputs. Raw ChIP-sequencing data is publicly available as GSE198026. (B) Validation of the top ranked H3K4me3, H3K27me3 and doubly-marked genes using quantitative real time polymerase chain reaction (qRT-PCR) in vector control (VCon), wild-type REIIBP and SET mutant REIIBP (R357Q). Mutant REIIBP had little changes on the expression of REIIBP differentially regulated genes when compared to control. Experiments were performed for 3 biological repeats with technical duplicates. Asterisks represent significant differences (**P*<0.05; ***P*<0.01, Student's *t* test).

that eIF3E increases TLR7 and BTK (*Online Supplementary Figure S9G*), we determined whether this was attributed to eIF3E canonical function as an initiator of protein synthesis. Using the analog O-propargyl-puromycin (OPP) that incorporates into newly synthesised proteins and coupled with florescence microscopy, there were no obvious differences between control and REIIBP cells in the number or rate of protein synthesis (Figure 8B). This was confirmed with the SUnSET protocol for immunoblot analysis of translation using puromycin-labeled proteins. Again, we did not detect significant differences in bulk protein translation with REIIBP (Figure 8B). More recently, eIF3 complex members have been implicated as RNA-binding protein (RBP), leading us to postulate that eIF3E might bind to the 3'UTR mRNA of oncogenic factors, known to increase mRNA stability and translation. In an RNA immunoprecipitation assay (RIP), we showed a direct interaction between *eIF3E and TLR7* mRNA, and to a lesser extent, BTK (Figure 8C). Polysome profiling indicated that TLR7 was efficiently translated by associating with polysomes found in the higher fractions in REIIBP cells as compared to control (Figure 8D; *Online Supplementary Figure S10*). Altogether, we revealed the mechanism of how eIF3E was epigenetically regulated by REIIBP, and its subsequent role in the translational status of TLR7.

Discussion

Alternative splicing events and promoter transcription start sites are major contributors to isoform diversity, giving rise to functionally different protein products from the same gene locus, a phenomenon common for oncogenes. *NSD2* is amongst the genes that has been demonstrated to produce multiple transcripts. However, the mechanism of how each transcript contributed to myeloma phenotype remains to be fully elucidated, since much of the research were focused on full-length *NSD2* as the predominant isoform. Little is known about the oncogenic function and therapeutic po-

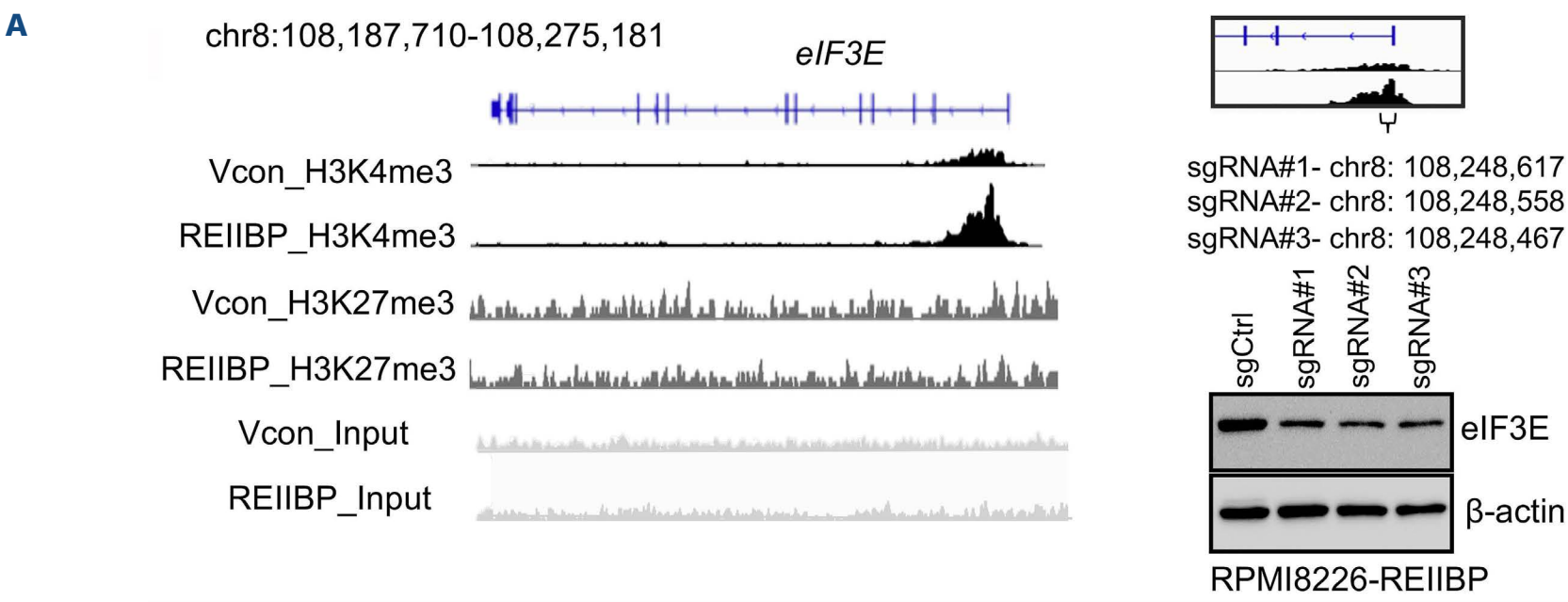

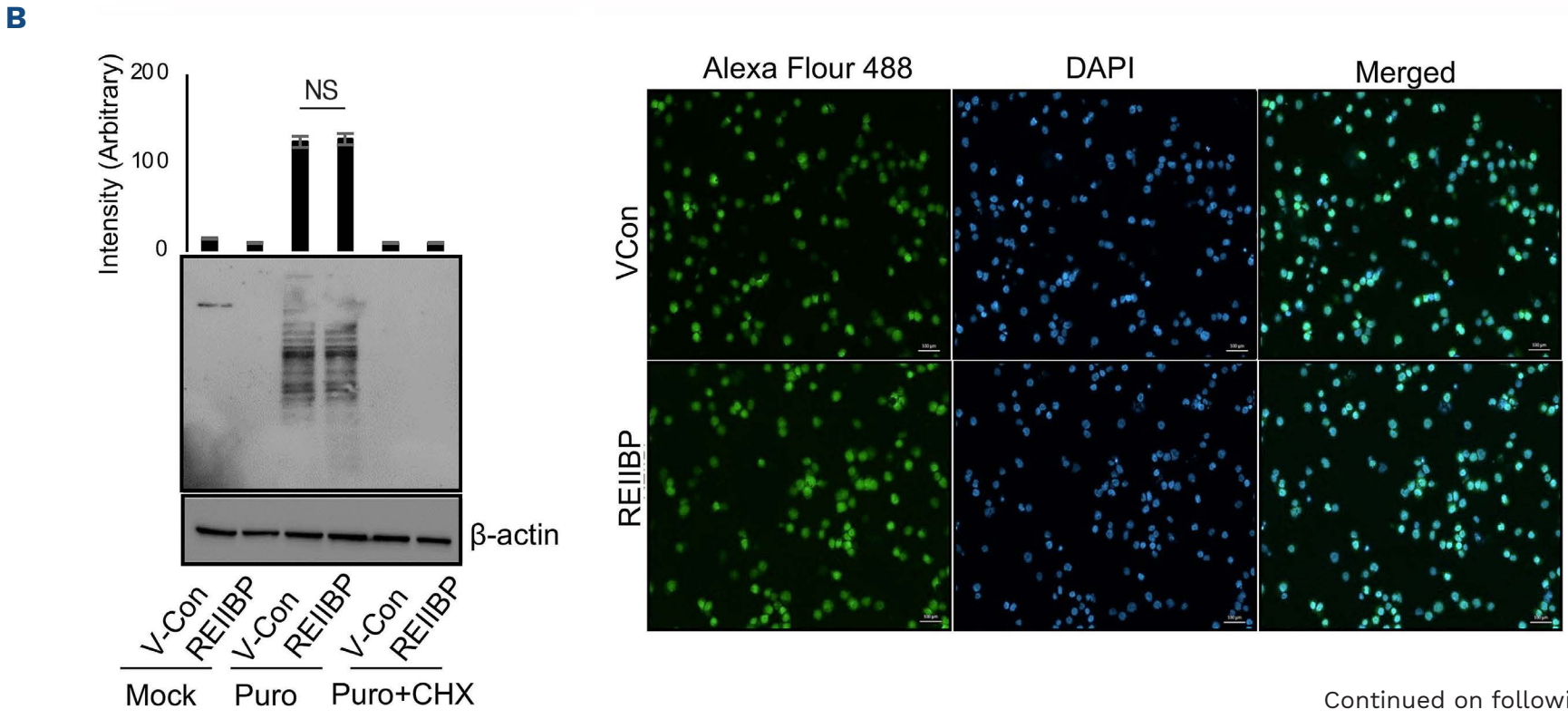

Continued on following page.

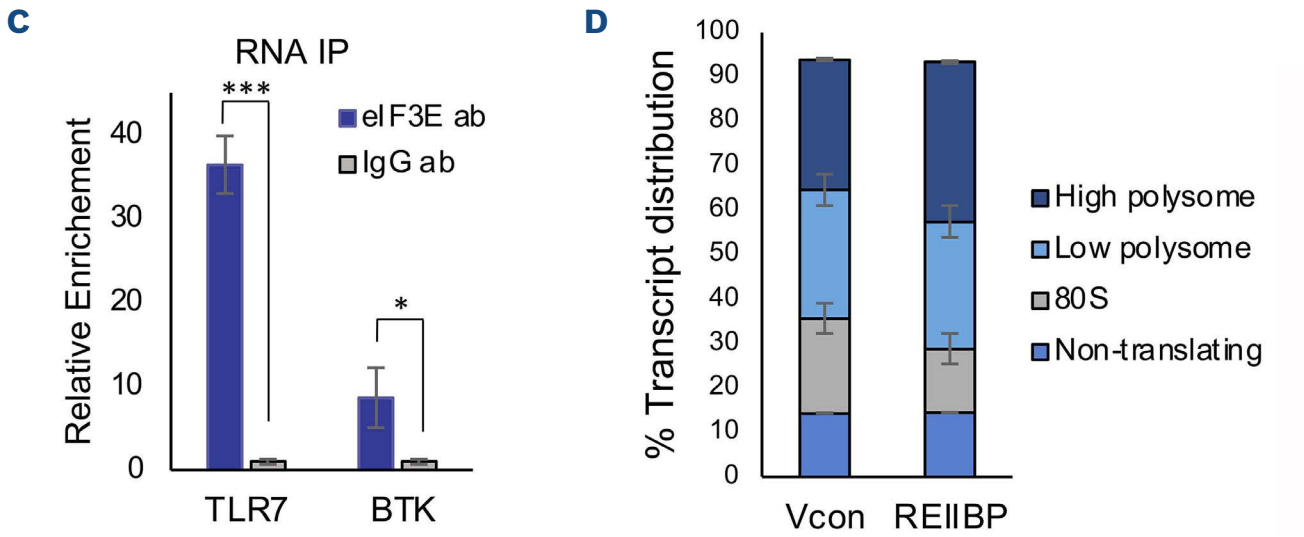

Figure 8. RNA-binding protein eIF3E was dysregulated by histone methylation and participates in REIIBP oncognesis. (A) Integrative Genomics Viewer (IGV) browser of representative gene tracks from biological triplicates of eIF3E were shown for H3K4me3 and H3K27me3 histone marks in RPMI8226-vector control (VCon) and RPMI8226-REIIBP cells. CRISPR/Cas9-mediated knockdown of H3K4me3 peak using 3 different single guide RNA (sgRNA) in RPMI8226-REIIBP cells with the positions of the sgRNA indicated. β-actin is the loading control. N=2, independent repeats, representative western blots (WB) shown. (B) Left panel: the global protein synthesis rate was determined by puromycin labeling[50] coupled with immunoblot using antibody against puromycin (12D10). Lanes 1 and 2 are mock treated, lanes 3 and 4 are labeled with 10 μg/mL of puromycin for 10 minutes and lanes 5 and 6 are labeled with puromycin and treated with 100 μM cycloheximide (CHX) for 10 minutes. Right panel: O-propargyl-puromycin (OPP)-labeling coupled with immunofluorescence in RPMI8226-VCon and RPMI8226-REIIBP. Newly synthesized proteins were stained with Alexa Flour 488 (green) and nucleus stained with DAPI (blue). Image is representative field. Scale bar, 100 μm. (C) RNA immunoprecipitation (RNA IP) was performed with eIF3E antibodies or immunoglobuolin (Ig)G control, and binding with *TLR7* or *BTK* mRNA was determined using quantitative real time polymerase chain reaction. Asterisks represent significant differences (*P<0.05; ***P<0.001, Student's t test). (D) The % transcript distribution of *TLR7* mRNA was determined in the non-translating, 80S, low polysome and high polysome after polysome profiling[51] comparing between RPMI8226-VCon and RPMI8226-REIIBP; 56.2% of *TLR7* mRNA were associated with polysomes as compared to 64.4% in REIIBP, indicating a higher translation efficiency in REIIBP cells.

tential of targeting REIIBP, due to the inability to perform REIIBP knockdown studies owing to a significant amount of overlapping gene sequences with *NSD2*, and the absence of a specific REIIBP antibody. In order to overcome these technical difficulties, we created a stable isogenic REIIBP cell line using RPMI8226, which expresses negligible levels of NSD2 isoforms. We elaborated on the molecular mechanism regulating REIIBP expression, which was not only driven by chromosomal rearrangement, but also EZH2-mediated miRNA gene silencing. Our observations corroborated a previous study that implicated EZH2 as an upstream regulator of NSD2 via its 3'UTR,[26] which is identical between REIIBP and NSD2. This supports the notion that most histone modifying enzymes do not work singly, but in a concerted effort to remodel the chromatin and alter transcription.[38,39] Here, we also uncovered a cooperative network consisting of several epigenetic regulators in t(4;14) MM.

One major finding is that despite homology between REIIBP and NSD2, the most prominent histone methylation activity of REIIBP is distinct from NSD2. REIIBP preferentially modifies H3K27me3 and H3K4me3, with minimal effect on H3K36me2, the primary modification by NSD2. These differences in histone substrates might undermine the efficacy of targeting SET domain specificities for clinical application. Given that the SET domain of REIIBP and NSD2 are identical, a reasonable interpretation could be differences in its subcellular localization or protein interacting partners, both of which can be caused by the absence of N-terminus sequences in REIIBP. Our results also further emphasize the promiscuity of the SET domain, which is supported by other literature based on the observed catalytic activity of NSD2.[12-15,40-41] Traditionally, EZH2 is the only known histone methyltransferase that catalyzes H3K27me3. Hence, we considered the possibility that REIIBP might indirectly regulate H3K27me3 levels through EZH2 or H3K27 demethylase JMJD3; but neither were dysregulated by REIIBP. Instead, a series of *in vitro* and *in vivo* experiments affirms that REIIBP have innate H3K27 methylation capabilities. The accumulation of H3K27me3 by REIIBP, which is associated with a closed chromatin state and transcriptional repression, was generally reflected in our microarray data where we saw more downregulated genes. H3K4me3 opposes the role of H3K27me3 by predominantly marking active promoters. In a bivalent domain, the co-occurrence of these two histone marks has been reported in embryonic stem cells as a mechanism to poise developmental genes for timely activation.[42] However, we did not observe true bivalent promoters since H3K4me3 was found near the TSS, while H3K27me3 was broadly distributed throughout the intergenic region. Our genomic analyses further suggested that the presence of H3K27me3 at gene loci is generally correlated with repression of gene expression, even prevailing over genes containing a high level of H3K4me3 for transcriptional initiation by RNA polymerase II. Our data also unexpectedly revealed an epigenetic regulation of RBP in MM, which are more commonly known to be dysregulated

through mutations or gene amplifications.[43] As RBP are involved in numerous RNA processing steps, their abnormalities have significant effects on post-transcriptional regulation and transcriptomes.[44]

Owing to the differences in histone preferences, it was within our expectations that we found little overlap of the differentially regulated genes between REIIBP and NSD2. Here, we uncovered a novel mechanism of BTK activation that bypasses BCR by REIIBP. BTK is a critical component of BCR signaling and a potent B-cell survival factor, but BCR is lost when B cell matures into plasma cells.[45] Intriguingly, BTK is re-expressed in MM, and we found that upregulation of TLR7 by REIIBP could represent a novel, important mechanism of BTK reactivation. Moreover, TLR7 was not expressed in the plasma cells from healthy donors,[29] making it possible to target cancer cells while sparing normal cells. We further reasoned that TLR- or BCR-mediated BTK activity could elicit differential downstream effects. Probing for all the effectors of BTK signaling identified a NF-κB-driven production and secretion of a key pro-inflammatory cytokine IL-6. Myeloma cells are highly dependent on the bone marrow tumor microenvironment and especially IL-6 for growth and survival, and the elevated expression of IL-6 is deemed a contributing factor for drug resistance.[46-48] This was reflected in patients who expressed high REIIBP levels and exhibited poorer response towards bortezomib, even when t(4;14) translocation is generally perceived to be responders towards bortezomib treatment. It also rendered REIIBP cells addiction to BTK signaling and targetability using Ibrutinib, a Food and Drug Administration-approved drug, and can be considered in combinational regimes to improve bortezomib response. Altogether, this study demonstrated that REIIBP is a functional histone methyltransferase in t(4;14) myeloma, and integrative analysis unraveled a eIF3E/TLR7/BTK axis that constitutes a targetable transcriptome driven by REIIBP epigenetic reprogramming in myeloma cells.

Disclosures

No conflicts of interest to disclose.

Contributions

PSYC and JYC designed the study and performed the experiments, analyzed and interpreted data. PSYC prepared the manuscript. PSYC and THC did the bioinformatics analyses. THC and RB did the ChIP-seq analysis. LSLJ, ALCY, MIBA and ZW did the in vitro work. SHMT and KB did the mouse work. NS and LAV did polysome profiling. WJC initialized the study, provided study directions, proofread and finalized the manuscript.

Acknowledgments

We thank Dr Frank Eisenhaber for insightful discussions on HMT assays. We thank Dr Xie Zhigang for his involvement in the conceptualization of the project. We thank Dr Zhou Jianbiao for advice on the in vivo mouse work.

Funding

WJC is supported by NMRC Singapore Translational Research (STaR) Investigatorship. This research was partly supported by the National Research Foundation Singapore and the Singapore Ministry of Education under the Research Centers of Excellence initiative as well as the RNA Biology Center at the Cancer Science Institute of Singapore, NUS, as part of funding under the Singapore Ministry of Education's Tier 3 grants, grant no. MOE2014-T3-1-006.

Data-sharing statement

Microarray data is provided as Online Supplementary Table S1. A list of genes with differential occupancy of H3K27me3 and H3K4me3 between RPMI8226-VCon and RPMI8226-REIIBP is provided as Online Supplementary Table S2. ChIP-sequencing data from this study were submitted to NCBI GEO (http://www.ncbi.nlm.nih.gov/geo/) under accession number GSE198026. The data analyzed in this study were obtained from MMRF CoMMpass Study at https://research.themmrf.org/.

References

1. Palumbo A, Anderson K. Multiple myeloma. N Engl J Med. 201;364(11):1046-1060.
2. Lu S, Wang J. The resistance mechanisms of proteasome inhibitor bortezomib. Biomark Res. 2013;1(1):13.
3. Quach H, Ritchie D, Stewart AK, et al. Mechanism of action of immunomodulatory drugs (IMiDS) in multiple myeloma. Leukemia. 2010;24(1):22-32.
4. Raedler LA. Darzalex (daratumumab): first anti-CD38 monoclonal antibody approved for patients with relapsed multiple myeloma. Am Health Drug Benefits. 2016;9(Spec Feature):70-73.
5. Fonseca R, Bergsagel PL, Drach J, et al. International Myeloma Working Group molecular classification of multiple myeloma: spotlight review. Leukemia. 2009;23(12):2210-2221.
6. Chng WJ, Glebov O, Bergsagel PL, Kuehl WM. Genetic events in the pathogenesis of multiple myeloma. Best Pract Res Clin Haematol. 2007;20(4):571-596.
7. Chng W, Dispenzieri A, Chim C, et al. IMWG consensus on risk stratification in multiple myeloma. Leukemia. 2014;28(2):269-277.
8. Hideshima T, Mitsiades C, Tonon G, Richardson PG, Anderson KC. Understanding multiple myeloma pathogenesis in the bone marrow to identify new therapeutic targets. Nat Rev Cancer. 2007;7(8):585-598.
9. Keats JJ, Maxwell CA, Taylor BJ, et al. Overexpression of transcripts originating from the NSD locus characterizes all t(4;14)(p16;q32)-positive multiple myeloma patients. Blood. 2005;105(10):4060-4069.
10. Brito JL, Walker B, Jenner M, et al. NSD deregulation affects cell cycle progression and adhesion regulons in t(4;14) myeloma plasma cells. Haematologica. 2009;94(1):78-86.
11. Kuo AJ, Cheung P, Chen K, et al. NSD2 links dimethylation of histone H3 at lysine 36 to oncogenic programming. Mol Cell. 2011;44(4):609-620.

12. Pei H, Zhang L, Luo K, et al. NSD regulates histone H4K20 methylation and 53BP1 accumulation at DNA damage sites. Nature. 2011;470(7332):124-128.
13. Popovic R, Martinez-Garcia E, Giannopoulou EG, et al. Histone methyltransferase NSD/NSD2 alters EZH2 binding and reprograms the myeloma epigenome through global and focal changes in H3K36 and H3K27 methylation. PLoS Genet. 2014;10(9):e1004566.
14. Lhoumaud P, Badri S, Rodriguez-Hernaez J, et al. NSD2 overexpression drives clustered chromatin and transcriptional changes in a subset of insulated domains. Nat Commun. 2019;10(1):4843.
15. Martinez-Garcia E, Popovic R, Min D-J, et al. The NSD histone methyl transferase switches global histone methylation and alters gene expression in t(4;14) multiple myeloma cells. Blood. 2011;117(1):211-220.
16. Lauring J, Abukhdeir AM, Konishi H, et al. The multiple myeloma-associated NSD gene contributes to cellular adhesion, clonogenic growth, and tumorigenicity. Blood. 2008;111(2):856-864.
17. Brito JLR, Walker B, Jenner M, et al. NSD deregulation affects cell cycle progression and adhesion regulons in t(4;14) myeloma plasma cells. Haematologica. 2009;94(1):78-86.
18. Xie Z, Chooi JY, Toh SHM, et al. NSD I acts as an oncoprotein and regulates GLO1 expression in t(4;14) multiple myeloma cells. Leukemia. 2019;33(3):739-748.
19. Garlisi CG, Uss AS, Xiao H, et al. A unique mRNA initiated within a middle intron of WHSC1/NSD encodes a DNA binding protein that suppresses human IL-5 transcription. Am J Respir Cell Mol Biol. 2001;24(1):90-98.
20. Nishioka K, Chuikov S, Sarma K, et al. Set9, a novel histone H3 methyltransferase that facilitates transcription by precluding histone tail modifications required for heterochromatin formation. Genes Dev. 2002;16(4):479-489.
21. Chu L, Su MY, Maggi LB Jr, et al. Multiple myeloma-associated chromosomal translocation activates orphan snoRNA ACA11 to suppress oxidative stress. J Clin Invest. 2012;122(8):2793-2806.
22. Mirabella F, Wu P, Wardell CP, et al. NSD is the key molecular target in t(4;14) myeloma. Blood Cancer J. 2013;3(5):e114.
23. Fingerman IM, Du HN, Briggs SD. In vitro histone methyltransferase assay. CSH Protoc. 2008;2008:pdb.prot4939.
24. Morey L, Helin K. Polycomb group protein-mediated repression of transcription. Trends Biochem Sci. 2010;35(6):323-332.
25. Feng Q, Wang H, Ng HH, et al. Methylation of H3-lysine 79 is mediated by a new family of HMTases without a SET domain. Curr Biol. 2002;12(12):1052-1058.
26. Asangani IA, Ateeq B, Cao Q, et al. Characterization of the EZH2-NSD histone methyltransferase regulatory axis in cancer. Mol Cell. 2013;49(1):80-93.
27. Gulati N, Béguelin W, Giulino-Roth L. Enhancer of zeste homolog 2 (EZH2) inhibitors. Leuk Lymphoma. 2018;59(7):1574-1585.
28. Chong PSY, Chooi JY, Lim JSL, Toh SHM, Tan TZ, Chng WJ. SMARCA2 is a novel interactor of NSD2 and regulates prometastatic PTP4A3 through chromatin remodeling in t(4;14) multiple myeloma. Cancer Res. 2021;81(9):2332-2344.
29. Bohnhorst J, Rasmussen T, Moen S, et al. Toll-like receptors mediate proliferation and survival of multiple myeloma cells. Leukemia. 2006;20(6):1138-1144.
30. Page TH, Urbaniak AM, Espirito Santo AI, et al. Bruton's tyrosine kinase regulates TLR7/8-induced TNF transcription via nuclear factor-κB recruitment. Biochem Biophys Res Commun. 2018;499(2):260-266.
31. Shinners NP, Carlesso G, Castro I, et al. Bruton's tyrosine kinase mediates NF-κB activation and B cell survival by B cell-activating factor receptor of the TNF-R family. J Immunol. 2007;179(6):6369.
32. Viatour P, Merville MP, Bours V, Chariot A. Phosphorylation of NF-kappaB and IkappaB proteins: implications in cancer and inflammation. Trends Biochem Sci. 2005;30(1):43-52.
33. Weber AN, Bittner Z, Liu X, Dang T-M, Radsak MP, Brunner C. Bruton's tyrosine kinase: an emerging key player in innate immunity. Front Immunol. 2017;8:1454.
34. Wang ML, Rule S, Martin P, et al. Targeting BTK with ibrutinib in relapsed or refractory mantle-cell lymphoma. N Engl J Med. 2013;369(6):507-516.
35. Rushworth SA, Bowles KM, Barrera LN, et al. BTK inhibitor ibrutinib is cytotoxic to myeloma and potently enhances bortezomib and lenalidomide activities through NF-κB. Cell Signal. 2013;25(1):106-112.
36. Ma J, Gong W, Liu S, et al. Ibrutinib targets microRNA-21 in multiple myeloma cells by inhibiting NF-κB and STAT3. Tumour Biol. 2018;40(1):1010428317731369.
37. Murray MY, Zaitseva L, Auger MJ, et al. Ibrutinib inhibits BTK-driven NF-κB p65 activity to overcome bortezomib-resistance in multiple myeloma. Cell Cycle. 2015;14(14):2367-2375.
38. Fischle W, Wang YM, Allis CD. Histone and chromatin cross-talk. Curr Opin Cell Biol. 2003;15(2):172-183.
39. Lee JS, Smith E, Shilatifard A. The language of histone crosstalk. Cell. 2010;142(5):682-685.
40. Kim JY, Kee HJ, Choe NW, et al. Multiple-myeloma-related WHSC1/NSD isoform RE-IIBP is a histone methyltransferase with transcriptional repression activity. Mol Cell Biol. 2008;28(6):2023-2034.
41. Woo Park J, Kim KB, Kim JY, Chae YC, Jeong OS, Seo SB. RE-IIBP methylates H3K79 and induces MEIS1-mediated apoptosis via H2BK120 ubiquitination by RNF20. Sci Rep. 2015;5:12485.
42. Voigt P, Tee WW, Reinberg D. A double take on bivalent promoters. Genes Dev. 2013;27(12):1318-1338.
43. Wang ZL, Li B, Luo YX, et al. Comprehensive genomic characterization of RNA-binding proteins across human cancers. Cell Rep. 2018;22(1):286-298.
44. Qin H, Ni H, Liu Y, et al. RNA-binding proteins in tumor progression. J Hematol Oncol. 2020;13(1):90.
45. Hendriks RW, Yuvaraj S, Kil LP. Targeting Bruton's tyrosine kinase in B cell malignancies. Nat Rev Cancer. 2014;14(4):219-232.
46. Chong PSY, Zhou J, Lim JSL, et al. IL6 promotes a STAT3-PRL3 feedforward loop via SHP2 repression in multiple myeloma. Cancer Res. 2019;79(18):4679-4688.
47. Chong PSY, Chng WJ, de Mel S. STAT3: a promising therapeutic target in multiple myeloma. Cancers (Basel). 2019;11(5):731.
48. Harmer D, Falank C, Reagan MR. Interleukin-6 interweaves the bone marrow microenvironment, bone loss, and multiple myeloma. Front Endocrinol (Lausanne). 2019;9:788.
49. Huang DW, Sherman BT, Lempicki RA. Systematic and integrative analysis of large gene lists using DAVID Bioinformatics Resources. Nature Protoc. 2009;4(1):44-57.
50. Schmidt EK, Clavarino G, Ceppi M, Pierre P. SUnSET, a nonradioactive method to monitor protein synthesis. Nat Methods. 2009;6(4):275-277.
51. Rahim AB, Vardy LA. Analysis of mRNA translation rate in mouse embryonic stem cells. Methods Mol Biol. 2016;1341:143-155.